Biol. Cybern. 68: 393–407 (1993)

Biological Cybernetics
© Springer-Verlag 1993

Rapid synchronization through fast threshold modulation

David Somers, Nancy Kopell

Department of Cognitive and Neural Systems and Department of Mathematics, Boston University, 111 Cummington Street, Boston, MA 02215, USA

Received: 6 February 1992/Accepted in revised form: 8 September 1992

Abstract. Synchronization properties of locally coupled neural oscillators were investigated analytically and by computer simulation. When coupled in a manner that mimics excitatory chemical synapses, oscillators having more than one time scale (relaxation oscillators) are shown to approach synchrony using mechanisms very different from that of oscillators with a more sinusoidal waveform. The relaxation oscillators make critical use of fast modulations of their thresholds, leading to a rate of synchronization relatively independent of coupling strength within some basin of attraction; this rate is faster for oscillators that have conductance-based features than for neural caricatures such as the FitzHugh–Nagumo equations that lack such features. Computer simulations of one-dimensional arrays show that oscillators in the relaxation regime synchronize much more rapidly than oscillators with the same equations whose parameters have been modulated to yield a more sinusoidal waveform. We present a heuristic explanation of this effect based on properties of the coupling mechanisms that can affect the way the synchronization scales with array length. These results suggest that the emergent synchronization behavior of oscillating neural networks can be dramatically influenced by the intrinsic properties of the network components. Possible implications for perceptual feature binding and attention are discussed.

1 Introduction

Phaselocking is a common property of coupled nonlinear oscillators. In some biological situations, large collections of oscillators appear to be able to come into synchrony very quickly, i.e., within a couple of cycles. This is true, for example, of synchrony between cells in the visual cortex when presented with certain kinds of stimuli (Eckhorn et al. 1988; Gray et al. 1989; Gray and Singer 1989). It is known that for some simple and widely-used caricatures of oscillators and coupling between them, locking in a long chain requires many cycles before transients disappear (Baldi and Meir 1990; Niebur et al. 1991; Schuster and Wagner 1990). It has therefore been suggested that the fast synchronization in distributed systems of oscillators *requires* coupling that is nonlocal (Kammen et al. 1989).

This paper analyzes a mechanism for achieving synchrony which has properties different from the synchronization mechanisms at work in the above caricatures, and which depends on properties of the oscillators. We work with oscillators and coupling that have well-known features common to typical models of neural oscillators or oscillating neural networks. The oscillators that we have in mind have more than one time scale, with transitional regions in phase-space. The coupling acts mainly to modify the position of the transitional regions, and we refer to this effect as "fast threshold modulation" or FTM. For such oscillators we show that for sufficiently close initial conditions, the properties of the oscillators determine the rate of approach to synchrony of a pair, almost independent of the size of the coupling; we contrast this with the behavior of phase models (Baldi and Meir 1990; Kammen et al. 1989; Kopell and Ermentrout 1986; Niebur et al. 1991; Schuster and Wagner 1990), in which the coupling is through "phase-pulling". In some limiting cases, synchrony for FTM is only marginally stable, rather than asymptotically stable, and we describe conditions necessary for asymptotic stability.

The mechanism responsible for the synchronization of a pair of oscillators also affects the emergent behavior of a chain of such oscillators. Using computer simulations and heuristic arguments, we show that a one-dimensional array using fast threshold modulation can synchronize much faster than such an array using a phase-pulling mechanism. We achieve rapid

Supported in part by NASA (NGT-50497)
Supported in part by NSF (DMS-8901913), and NIMH-47150
Present address and address for correspondence: Department of Brain and Cognitive Sciences, Massachusetts Institute of Technology, E25-618, Cambridge, MA 02139, USA

synchronization using only nearest neighbor connections, which is consistent with other recent modeling work (Grossberg and Somers 1991; König and Schillen 1991) that had appeared to be in direct conflict with theoretical and simulation results for phase difference coupling (Baldi and Meir 1990; Kammen et al. 1989; Niebur et al. 1991; Schuster and Wagner 1990). This paper resolves the apparent conflict between these two sets of results and in so doing establishes an important caveat for researchers attempting to construct network architectures that exhibit synchronization: intrinsic properties of the oscillatory network components can significantly affect the synchronization properties achieved for a given connective architecture.

The paper is organized as follows. In Sect. 2, we give the general form of the oscillators and their interactions that we call Fast Threshold Modulation. For the sake of comparison, we also discuss interaction of phase oscillators coupled via phase differences. For FTM, we discuss how trajectories starting in different regions of phase space are brought close together, and what properties of the oscillators make this process most efficient. The key notion is "rate of compression", which measures relative velocities of the slow variable just before and just after a fast jump of the oscillator. We also show that some caricatures (but not realistic ones) of these oscillators may not synchronize stably; instead there is a one-parameter family of periodic solutions with different periods. If the fast time scale is not infinitely fast with respect to the slow variable, the oscillators first aggregate quickly into a state of approximate or "noisy" synchrony, then go to synchrony on a slower time scale. Our results are summarized in a theorem. These abstract ideas imply predictions about specific oscillators. We show, using analysis, that conductance-based Morris–Lecar oscillators (1981) synchronize much more quickly than the caricature oscillators of FitzHugh (1961) and Nagumo et al. (1962). We also give reasons why conductance-based models can in general be expected to do better than caricatures such as FitzHugh–Nagumo.

In Sect. 3, we present computer simulation results for locally coupled one-dimensional arrays of oscillators. In addition to the single cell Morris–Lecar oscillator model, we introduce a network-based oscillator model due to Ellias and Grossberg (1975). With either the single cell or the network-based oscillators we were able to compare the synchronization rate of arrays of relaxation oscillators with that of sinusoidal arrays. This was accomplished by varying the relative internal time scales of the oscillators. Our results show that for a wide range of initial conditions and coupling strengths that relaxation arrays synchronize in many fewer cycles than sinusoid arrays, under similar conditions. We present heuristic explanations of this effect based on the scaling properties of the FTM mechanism and of phase difference coupling.

In the last section we summarize some main points and discuss related points. One such point is why oscillators coupled through a FTM mechanism are not necessarily well described by models involving pulse coupling. Another involves potential implications of our findings for perceptual feature binding in visual cortex.

2 Mechanisms of synchronization: fast threshold modification and phase-pulling

The oscillations we shall analyze can be described by equations of the form

$$\begin{aligned} \epsilon\, dx/dt &= f(x, y, I)\,, \\ dy/dt &= g(x, y)\,, \end{aligned} \tag{1}$$

where, for a range of I, $f(x, y, I) = 0$ can be solved for $y = F(x; I)$ and the latter has a cubic shape. As in Fig. 1, for $\epsilon \ll 1$ the periodic orbit in the phase-plane diagram of (1) hugs the extreme branches of the nullcline along the slow portion of the cycle. The parameter I plays the role of an injected current in single cell models, and excitatory input in the case of network models.

Now consider a pair of oscillators, each described by (1), where the second oscillator has variables $\hat{x}, \hat{y}$. The coupling (which we shall refer to as "Heaviside coupling") is done by making I a function of the fast variable of the other oscillator to which it is coupled. We require that $I(\hat{x})$ be constant along each of the two branches (right and left) of the limit cycle of (1), with a higher value on the right hand branch (RHB) with larger $\hat{x}$. Let I^- and I^+ denote these two values. We also require that $y = F(x; I)$ be an increasing function of I for each x, so that increasing the value of I raises the nullcline $f(x, y, I) = 0$, perhaps with change of

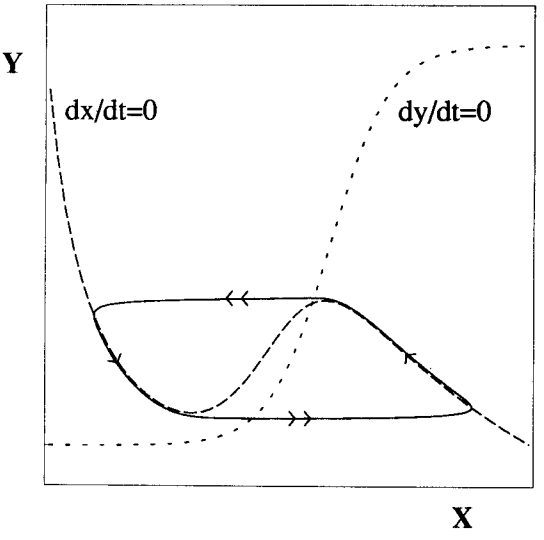

Fig. 1. Phase-plane diagram of the periodic orbit and nullclines of the relaxation form ($\epsilon \ll 1$) for a system described by equations (1). The periodic orbit consists of two slow regions alternating with two fast regions: the trajectory moves slowly near the outer branches of the cubic-like nullcline to the local extremum or "knee" of the cubic branch, at which point the trajectory rapidly jumps to near the other branch

shape. The equations satisfied by each oscillator are determined by the branch on which the second oscillator is travelling, which determines the value of I in (1). We note that the coupling gives no information about the position of the oscillator on its branch. In this sense, the oscillators are uncoupled between their jumps.

We may now investigate how trajectories of the coupled system having different initial conditions for the two oscillators develop as time increases. The analysis just below deals with "singular solutions", i.e., refers to the limiting case in which the jumps between branches take place infinitely fast. We will then discuss the modification for $\epsilon \neq 0$.

We first note that even when the oscillations are synchronous, the trajectory is not the same as that of a single uncoupled oscillator. Indeed, in all the examples we give in the next section, coupling that mimics excitatory coupling leads to a synchronous solution with lower frequency and higher amplitude. By the "limiting synchronous solution" (LSS) we mean the union of relevant pieces of the left hand branch (LHB) of the $(I = I^-)$ cubic, the RHB of the $(I = I^+)$ cubic, and the fast transitions between these regions (see Fig. 2).

Denote by k_L (resp. k_U) the lower knee of the lower cubic (respectively the upper knee of the upper cubic). The knees, or extrema of the cubics, represent thresholds for jumping to the other branch. Thus each oscillator in the relaxation regime has an onset threshold at the local minimum and an offset threshold at the local maxima. These extrema are changed by the coupling, and it is the local maxima and minima of the $I = I^-$ and $I = I^+$ cubics that will be relevant, not the thresholds for the uncoupled oscillators.

The analysis of the trajectories of the coupled system is divided into cases depending on the initial values of the two oscillators.

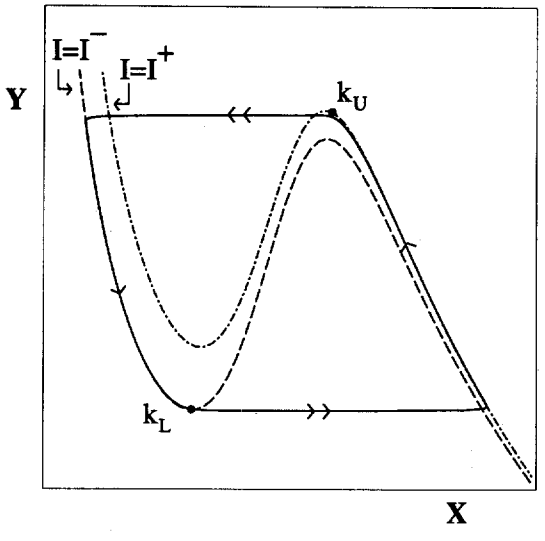

Fig. 2. Phase-plane trajectory of the limiting synchronous solution (LSS) of an excitatorily coupled pair of oscillators defined by (1). For the oscillators shown here (Morris–Lecar) with a sigmoidal coupling function, the trajectory closely follows the nullclines predicted by the Heaviside coupling hypothesis

1. The oscillators start on the same branch (i.e., both on the RHB or both on the LHB). In this case, the oscillators each move (at least initially) on a branch of the synchronous solution. That is, the input to each oscillator via the coupling is the same as that for the synchronous oscillators.
2. The oscillators start on opposite branches.

We begin with case 1, which we separate further into subcases. By appropriate choice of the origin in time, we may assume that one of the two oscillators (called "oscillator 1") is at k_L or k_U; for definiteness, we assume it is at k_L. The subcases are as follows:

1a. If oscillator 2 is "sufficiently close" in initial condition, the jump of oscillator 1 causes oscillator 2 to also jump immediately, with oscillator 2 now leading on the RHB (see Fig. 3a). The larger the shift of the cubic, the larger the modulation of the threshold, and thus the larger the range of initial conditions that fall into this case.
1b. For larger differences in the initial conditions, the jump of oscillator 1 does not immediately cause a jump for oscillator 2. It changes the trajectory of oscillator 2 to a different nullcline, for which the jump threshold is nearer. In this range of initial conditions for oscillator 2, the order of the two oscillators still reverses once oscillator 2 jumps (see Fig. 3b).
1c. For initial conditions still more distant from k_L, there is no order reversal between oscillators 1 and 2 on the RHB just after the jump of oscillator 2 has been made (see Fig. 3c).
1d. For some sufficiently distant initial conditions, oscillator 1 may return to the LHB before oscillator 2 jumps off the LHB.

We first show that threshold modulation, as above, is not enough to ensure that synchrony is asymptotically stable, i.e., that even in the limit $\epsilon \to 0$, differences need not decay. We do this by showing that trajectories with initial conditions in case 1a need not approach synchrony. Then we give conditions that ensure such stability.

Example: Consider a piecewise-linear caricature of (1) in which the oscillator travels at uniform speed along each branch until it reaches a corner and jumps; the length of the two branches are equal. The function I is 0 on the left outer branch and 1 on the right branch; when $I = 1$, the "cubic" is raised from its $I = 0$ position (see Fig. 4). For this version of (1), there is no approach to synchrony: if the initial conditions are within the size of the jump due to the change in I, the oscillators interchange lead at each jump, without decreasing the size of the difference between them. There is not even a unique solution for which the oscillators jump simultaneously (to possibly different values of the slow variable); there is a one-parameter family of solutions such as the one described above (parameterized by the difference in slow variable at the jump), and the frequency of the coupled pair varies substantially within this family.

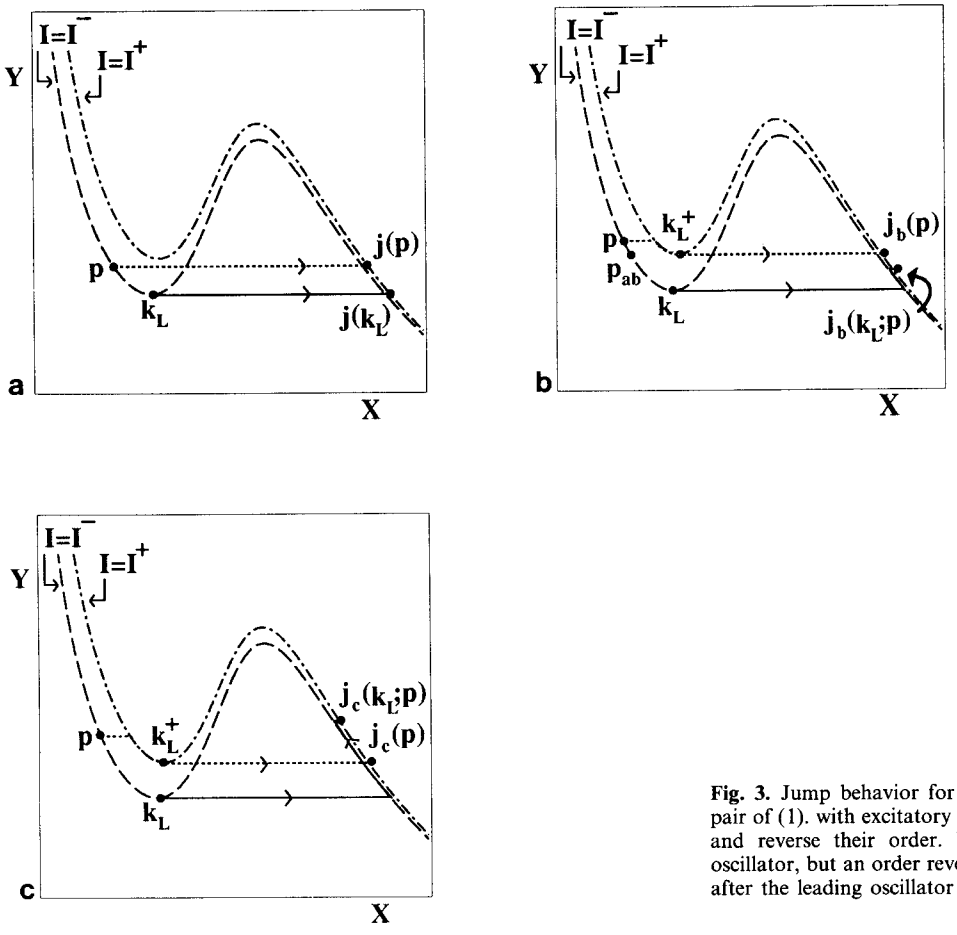

Fig. 3. Jump behavior for three subcases of initial conditions for a pair of (1). with excitatory coupling **a** oscillators jump simultaneously and reverse their order. **b** lagging oscillator jumps after leading oscillator, but an order reversal still occurs. **c** lagging oscillator jumps after the leading oscillator and order of the oscillators is unchanged

The above example shows that jumps and fast modulations of them need not produce an asymptotically stable synchronous solution. But under an additional condition, shared by more "realistic" models of neuronal oscillations, asymptotic stability is achieved. The additional condition is on pairs of points that satisfy case 1a.

Definition: Let p be a point on the left branch or right branch, close enough to the knee to be in case 1a. Let $j(p)$ be the point on the opposite branch for which the slow variable has the same value (i.e., $j(p)$ is the point to which a trajectory "jumps" from point p). Let $\tau(p)$ be the time along the LSS from p to the knee on its branch, and $\tau(j(p))$ the time along the LSS from j(knee) to $j(p)$. We define the compression $C(p)$ by

$$C(p) \equiv \tau(j(p))/\tau(p) .$$

Condition C: $C(p) < 1$ uniformly for points of type 1a.

Remarks:

2.1. This condition says that the time from point p to k_L exceeds the time between the points on the opposite branch having the same values of the slow variable. It is satisfied if the rate of change of the slow variable before the jump is less than that after the jump, for example, if graph of y vs. time has a "scalloped" shape, with $y' \cdot y'' < 0$ as in Fig. 5. (The opposite convexity yields an expansion).

2.2. The notion of compression is almost independent of coupling strength. (The latter, however, affects the size of the interval of points in case 1a.) More specifically, compression is dependent on the rates of the slow variable along the two branches of the LSS. These are close to the rates along the branches of the uncoupled oscillators. The degree to which compression is independent of coupling strength for points in case 1a depends on how much the velocity along the $I = I^-$ cubic differs from that along the $I = I^+$ cubic along the same branch (RHB or LHB). If we identify the uncoupled oscillator with the $I = I^-$ system (i.e., assume each oscillator gives off a coupling signal only when it is excited), then it is only the difference of the cubics on the excited branch that is relevant. For conductance-based models like Morris–Lecar (presented in Sect. 3), the RHB is changed much less for a given change in I than is the LHB. (For example, see Fig. 2.)

2.3. In the context of pulse coupled oscillators, Mirollo and Strogatz (1990) introduced a similar concavity

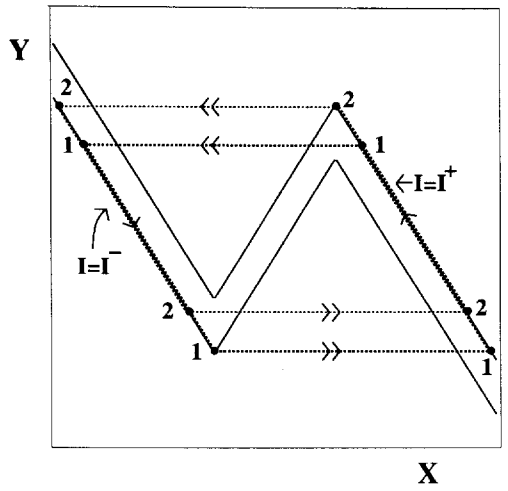

Fig. 4. Fast threshold modulation alone does not guarantee synchrony. In this piecewise linear caricature of (1) if the trajectories move at uniform speed along the outer branches, then an order reversal may occur during each jump but the phase difference between the oscillators will remain constant

condition to insure synchrony. When their concave function was replaced with a linear function the pulse coupled system also exhibited behavior analogous to that of the piecewise linear caricature shown above in Fig. 4; however, the pulse coupled model cannot explain the full range of effects that we observe here. These differences are discussed in Sect. 4.1.

As we show below, compression factors less than one lead to stable synchrony (for the solutions to the limiting equation), and the smaller the $C(p)$ (the stronger the compression), the faster the approach to synchrony. To show this, we first introduce a notion of phase difference. For coupled oscillators such as the ones described by (1), with coupling as above, there is no obvious notion of phase that is valid for all trajectories. The difficulty is that the jump of one oscillator effectively changes the phase space of the other; a notion like "time until the next jump" depends on the position of the other oscillator. However, since it depends only on the branch of the other oscillator, we can define phase difference whenever both trajectories are

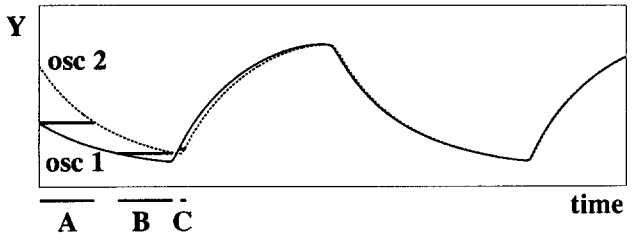

Fig. 5. "Scalloping" of slow variable (Y) time course determines phase compression. The phase difference between two oscillators lying along the same branch is determined by the time difference between their slow variables (see black bars). In the relaxation limit, phase changes occur only during the branch jumps which are represented by corners in the slow variable time course

on the same branch, using a notion of phase that comes from the LSS.

Definition: Let p and q be two points on the LSS. The phase difference from p to q is the ratio of the time it takes to go from p to q, divided by the period of the LSS.

The following proposition is now immediate from the definitions:

Proposition 2.1: *Suppose p is some point satisfying case* 1*a. Then* (*i*) *If $C(p) < 1$, the phase difference between p and k_L is reduced by a factor of $C(p)$ during the jump.* (*ii*) *Between jumps, there is no change of phase difference between two points on the same branch.* (*iii*) *Suppose that the phase-difference between $j(k_L)$ and $j(p)$ lies in case* 1*a, for the leftward jump at k_U. (The phase-difference is well-defined and constant until one of the two oscillators reaches k_U.) Then the trajectory of the coupled system, starting with oscillators at p and k_L, approaches synchrony with a geometric rate of attraction. A lower estimate of this rate is $\max\{C(p) \mid p$ is on the* LHB *satisfying case* 1*a for the righward jump, or p is on the* RHB *and satisfies case* 1*a for the leftward jump*$\}$.

Remarks:

2.4. The notion of phase difference depends on *time* difference along the trajectory, not differences in position in phase space. The phase space variables can appear to get closer as they move along a branch; this apparent (but not real) compression occurs if the rate of change of the slow variable decreases along the branch as in Fig. 5.

2.5. By part (*iii*) of the above proposition, a sufficient condition for a domain of asymptotic stability is that there is a uniform rate of compression (less than 1) near both corners, and that the points of type 1a for each of the jumps map to points close enough to the image of the corresponding knee that they are in the region where there is compression on the next jump. Neither of these hypotheses are necessary. If there is a large enough compression at one jump, there can even be some expansion at the other jump and maintain asymptotic stability. A weaker sufficient condition is that the image of the points of type 1a after two jumps (one rightward and one leftward) lies again in the region of type 1a and the composition map compresses phases.

We now consider initial conditions of the type 1b. We continue to assume condition C and assume for definiteness that the trajectory starts with two points on the LHB, one at k_L and the other at p. We develop a notion of compression for points p of type 1b.

Let $j_b(p)$ be the point on the RHB reached by oscillator 2 just after its jump (see Fig. 3b). During the time before this jump, oscillator 1 has been following a trajectory on the RHB. Let $j_b(k_L; p)$ be the point to which oscillator 1 arrives when oscillator 2 is at $j_b(p)$.

Let $\tau_b(p)$ be the time necessary to go from p to k_L along the LHB of the LSS, and $\tau_b(j(p))$ the time from $j_b(k_L; p)$ to $j_b(p)$. As before, the compression is defined to be

$$C_b(p) \equiv \tau_b(j(p))/\tau_b(p) .$$

Proposition 2.2: *Let p_{ab} denote the point on the boundary between points of types 1a and 1b. For p of type 1b, $0 \leqslant C_b(p) \leqslant C(p_{ab})$. Thus, a uniform estimate of compression for points of type 1a extends to a uniform estimate for points of types 1a and 1b.*

Proof: For $p = p_{ab}$, $C_b(p) = C(p)$. For p further from k_L, $j_b(p) = j(p_{ab})$ and $j_b(k_L; p)$ is higher on the right branch than $j(k_L)$. Hence $\tau_b(j(p))$ is smaller than $\tau(j(p_{ab}))$. As p approaches the upper boundary of points of type 1b, $\tau_b(j(p)) \to 0$. Thus, as p increases in distance from p_{ab} to the upper boundary, the numerator of $C_b(p)$ decreases to zero, while the denominator increases. Thus $C_b(p)$ decreases from $C(p_{ab})$ to 0 as p goes from p_{ab} to the upper boundary of points of type 1b. ■

Remark 2.6: The upper part of the region of type 1b, and parts of type 1c, may be thought of as "supercompressed", with points at a substantial distance mapped almost to the same point.

The compression properties of points of type 1c depend on details of the equations and the coupling. Points of type 1c may not exist. If they do, a compression ratio $C_c(p)$ may be defined analogously to $C_b(p)$. In this case, as p moves upward through the region of type 1c, the denominator of $C_c(p)$ increases, but so does the numerator. Since the numerator starts from 0, there is always a subregion in which $C_c(p) < 1$. To see that there may be points at which there is an expansion, we consider a potential "worst case": Let p be the highest point on the LHB of the LSS. Assuming that p is not of type 1a or 1b, either $j(k_L; p)$ is higher on the RHB than $j(p_{ab})$ (see Fig. 3c) or $j(k_L; p)$ is not well-defined. (The latter is true if oscillator 1 jumps back to the LHB before the initial jump of oscillator 2, so p is of type 1d.) If the latter holds, let p instead be the highest point of type 1c on the LHB. Between the jump of oscillator 1 and that of oscillator 2, the latter travels on the LHB of the $I = I^+$ cubic, not the cubic $I = I^-$ of the LSS. Note that the time in the numerator of $C_c(p)$ is also the time necessary to go along the LHB of this higher cubic from the point at height p down to the lower knee k_L^+ of this upper cubic. (The height of k_L^+ is the same as that of p_{ab}; see Fig. 3b). The denominator is the time necessary to go from p down to k_L, the lower knee of the lower cubic. Though the distance to k_L^+ is shorter, the trajectory is along a path for which the vertical velocity can be considerably smaller. (For the equations in Sect. 3, the vertical velocity on the LHB of the upper cubic is indeed smaller than that on the lower cubic; similarly the vertical velocity on the right branch of the LSS is larger than that of the RHB of the lower cubic.) Thus, without further hypotheses, one cannot say which of the two times is longer. However, when the speed of the slow variable does not differ dramatically between the upper and lower cubics, initial phase conditions of type 1c can be significantly compressed, possible yielding (as for the oscillators in Sect. 3) a greater absolute (but not relative) phase compression than types 1a or 1b. Unlike case 1a, the size of this phase compression does depend on the coupling strength.

Case 1d occurs when oscillator 1 traverses the right branch and returns to the left branch before oscillator 2 jumps to the right branch. Under these conditions, there can be a stable antiphase solution. Such solutions are discussed briefly in Sect. 4 and in rigorous detail in (Kopell and Somers 1993).

Initial conditions which belong to case 2 (opposite branches) generically will fall into case 1 after the next jump of either oscillator. If both jump simultaneously to opposite branches they will either fall into case 1 after one more jump of either oscillator or will exhibit (possibly unstable) anti-phase behavior.

Remark 2.7: The above discussion shows that there is a range of initial phase differences for which approach to synchrony is geometric, though synchrony need not be the only attractor. The degree of "scalloping" of the slow variable (as in Fig. 5) on the LSS determines the rate of attraction for the points in the basin of attraction. We point out here that a larger degree of scalloping helps synchronization efficiency in another way: Since an oscillator which exhibits stronger scalloping spends a larger fraction of its period just before the jumps, for a given coupling strength (i.e., a given change in the cubic nullcline), a larger fraction of points are of type 1a, in which the geometric compression occurs. Strong scalloping may also (but need not) increase the absolute phase compression in case 1c.

We now turn to modifications of this theory to deal with $\epsilon \neq 0$. We first note that there is no difficulty in proving the existence of a synchronous solution for ϵ sufficiently small: Replacing $(\hat{x}, \hat{y})$ by (x, y) in the coupled equations, we see that the synchronous solution satisfies a two-dimensional equation similar to, but not identical to that of the uncoupled oscillators. The usual arguments producing a periodic solution for two-dimensional relaxation oscillators then work in this case. Thus we can concentrate on approach to synchrony.

For $\epsilon \neq 0$, the analogue of $C(p)$ is as follows: Define $\tau_\epsilon(p)$ to be the time from p to the lowest point on the trajectory (for a rightward jump, and to the highest point for a leftward jump). Let $\tau_\epsilon(j(p))$ be the time from that extrema point to the point with the same value of the slow variable as $j(p)$. Define $C_\epsilon(p) \equiv \tau_\epsilon(j(p))/\tau_\epsilon(p)$.

Note that if $\tau(p)$ is bounded away from 0, then $C_\epsilon(p) \to C(p)$ as $\epsilon \to 0$. This is not true for points in a small interval around k_L. That is, for a sequence of points p_ϵ such that $\tau(p_\epsilon) \to 0$ as $\epsilon \to 0$, $C_\epsilon(p_\epsilon)$ does not

approach $C(p)$. This leads to a different time scale for synchronization of points that start very close to one another.

To understand the origin of the different (and generally slower) time scale, we consider coupling that is "pure Heaviside". By this we mean that I is a piecewise-constant function of $\hat{x}$, with its discontinuities strictly between the two branches of the LSS. It is well known (Mishchenko and Rozov 1980) that for relaxation oscillators, the time needed to traverse a slow branch is $O(1)$, and the time between branches is $O(\epsilon)$. In addition, there is a transitional region around the knee for which traversal occurs on an intermediate time scale. Consider a point p that is $O(\epsilon)$ in time from the lower knee of the synchronous solution. We shall show that a pair of oscillators with one trajectory at p and the other at the knee do approach synchrony geometrically, but the rate of approach is not the same as (or even a perturbation of) the $\epsilon = 0$ theory given above.

The piecewise constancy of I implies that the trajectory "senses" the non-synchrony only over that part of the trajectory for which the value of I is different for the two oscillators. This happens during both the rightward and the leftward jumps. For points $O(\epsilon)$ close, the transistions are the same; the two oscillators differ in coupling input only during a time interval of $O(\epsilon)$ when the points lie on opposite sides of the discontinuity of I. The ratio of their speeds over this time is $f(x, y, I^+)/f(x, y, I^-)$, a quantity that is essentially constant over that $O(\epsilon)$ period. Thus, over one period of the oscillators, the phase difference gets reduced by a factor between the minimum and maximum of the above ratio. A generalization of this argument yields the same conclusion for coupling that is not pure Heaviside, where I has a rapid but not necessarily instantaneous transition from I^- to I^+.

This shows that for points starting $O(\epsilon)$ apart, the approach to synchrony is geometric. Note however that the relevant compression factor uses data about velocities during the jump, not during the slow segments. Furthermore, the compression is much more dependent on coupling strength $(I^+ - I^-)$ than is the $\epsilon = 0$ compression. Also note that the former compression, though $O(1)$, is not very strong. For a 20% coupling (i.e., excitatory effect of the coupling input in the LSS equals 20% of the intrinsic excitatory component) of the Morris–Lecar oscillators (see Sect. 3), the above ratio of speeds in the central half of the jump is bounded by 0.8. This contrasts with compressions of $C = 0.1$ for the M–L oscillator in type 1a compression (see Remark 2.8). We believe that this pair of effects can help to account for the noisy synchrony slowly giving way to true synchrony seen in our simulations of arrays of oscillators (see result 6 of Sect. 3.3).

Finally, we note that for the initial phase differences of $O(\epsilon)$ there is no order reversal during the jump. Thus, over the transitional region in which the intermediate time scale operates, there is a change from order reversal to order preservation. This implies that some points starting apart get mapped onto the same value of the slow variable, as at the boundary between regions of type 1b and 1c. Thus, the time scales discussed above are not a complete description. Even for the points starting in the transitional region, the lagging oscillator always gains on the leading one whenever the two have differential input, so points starting close together do approach synchrony.

Many of the results of this section are summarized by the following:

Theorem: *Suppose that a pair of identical relaxation oscillators is coupled through a* FTM *mechanism, and Condition C is satisfied. Then*

1. *For the $\epsilon = 0$ limit, the synchronous solution has a domain of attraction in which the approach to synchrony is geometric. The set of points of types* 1a *and* 1b *give an underestimate of this domain. The rate of attraction is computed from the speed of the slow variables on the two branches of the* LSS, *quantities that vary little with coupling strength. The domain of attraction also includes some points of type* 1c, *for which the rate of attraction does depend on the coupling strength.*

2. *For $0 < \epsilon \ll 1$, there is a region in phase-space with the oscillators starting close together, in which the approach to synchrony is on a different time scale (or scales) from the above. For points differing initially by $O(\epsilon)$, the approach is again geometric, computed from speeds during the fast jumps. This rate is more sensitive to coupling strength.*

Remark 2.8: The general theory presented above yields computational methods for estimating the relative speed of approach to synchrony. In this remark we compare a single cell conductance-based model due to Morris and Lecar (1981) to a standard simplification of single cell conductance-based models due to FitzHugh (1961) and Nagumo et al. (1962). The latter equations are considered to be the simplest equations that embody the nonlinearity responsible for the excitable and/or oscillatory behavior of a space-clamped neuron. As shown below, the extra structure of the full conductance model makes the approach to synchrony much faster. The full Morris–Lecar equations and parameters are presented in Sect. 3.1. The FitzHugh–Nagumo (F–N) equations have the form

$$\begin{aligned} dv/dt &= f(v) - w + I_{\text{ext}}, \\ dw/dt &= \epsilon v, \end{aligned} \tag{2}$$

where $f(v) = v(b - cv^2)$, The parameters for (2) were chosen as $A = 2.67$, $B = 2.58$, $V = 17.15$, with I_{ext} ranging from 0 to 0.2 so that the F–N oscillations had the same amplitude, period, and voltage range as the M–L oscillations. In order to compare these two models, the coupling for both F–N and M–L was chosen to mimic excitatory chemical synaptic coupling and the same coupling form was used for both: add the term $-\alpha g_{CA} m_\infty(\hat{v})(v - 1)$ to the equation of both (2) and (4), where $\hat{v}$ is the voltage of the paired oscillator. Here α parameterizes the strength of the coupling input, and was varied across simulation trials.

According to the theory developed above, in the relaxation limit ($\epsilon \approx 0$) the rate of approach to synchrony can easily be computed numerically from the slow variable time course. The compression rate may be estimated in several ways. Analytically, a crude but rigorous upper bound on $C(p)$ is found by dividing the maximal vertical speed between a point p and k_L by the minimal vertical speed between $j(k_L)$ and $j(p)$. Geometrically, one can estimate the times $\tau(p)$ and $\tau(j(p))$ from the graph of the slow variable versus time on the synchronous trajectory. Note that the greater the scalloping of the slow variable, the more the compression. Under identical coupling and initial conditions, a 10% difference in phase between a pair of M–L oscillators can be compressed into just over a 1% phase difference in a single jump ($C \approx 0.1$), whereas F–N compresses only to a 6% phase difference ($C \approx 0.6$). M–L can compress a 25% phase difference into a 0.5% difference in a single cycle (2 jumps), but it would take F–N 4 cycles (8 jumps) to achieve the same compression. The slow variable scalloping also provides a synchronization advantage for M–L in cases 1b and 1c. Indeed, for all initial conditions tested, Morris–Lecar was better at synchronizing trajectories than was FitzHugh–Nagumo under the same coupling conditions.

This effect is not due to particularly well-chosen parameter values for M–L. Rather, the M–L equations have helpful features that are general to a large class of single cell conductance-based models. To see this, we consider the behavior of the slow variable in the relaxation limit. For both F–N and M–L, the rate of the slow variable (for a given fast variable value) depends on the difference between the slow variable value on the fast variable nullcline and the value on the slow variable nullcline. For F–N the slow variable nullcline is the vertical line $v = 0$, so the compression factor at a jump depends only on the shape of the cubic (fast) nullcline. However, for M–L the slow variable nullcline is S-shaped (see Fig. 1), approaching the fast variable nullcline near the jump thresholds and thus amplifying the compression. The slow variable rate of M–L also has a proportionality factor $\tau_w(v)$ which contributes a factor as small as 0.25 to the compression. These mathematical differences between M–L and F–N come from the differences in physical meaning: M–L models the conductance changes of the recovery variable, including the sigmoidal dependence on voltage, while F–N depends linearly on voltage and does not model the conductance kinetics.

Remark 2.9: To emphasize the ideas, we now compare the behavior with that of another class of coupled oscillators. In this caricature, the oscillator is described by a single variable, its phase θ. Under various circumstances (see Kopell and Ermentrout 1991), coupling among oscillators may be reduced to interactions dependent only on the differences between phases of the coupled oscillators. The most simple such coupling (though not one given generically by the reduction procedures) is given by the sine of the phase differences. If the oscillators all have the same frequency ω, the equation describing the jth oscillator is then

$$d\theta_j/dt = \omega + A \sin(\theta_{j+1} - \theta_j) + A \sin(\theta_{j-1} - \theta_j) . \quad (3)$$

In this case, the phase-locking is achieved by "phase pulling"; if either the $j+1$st or $j-1$st oscillator leads or lags the jth, it exerts a "force" that locally changes the frequency of the jth in a direction to decrease the phase differences between the oscillators. This force is an increasing function of the phase difference, so an oscillator whose phase is far away exerts a stronger influence on a given oscillator than one whose phase is closer. (It is not hard to establish that, except for some special initial conditions, the synchronous state is globally attracting.)

The phase pulling mechanism contrasts with the FTM mechanism in several ways:
(a) The FTM coupling has an effect only at the jumps; phase pulling acts continuously along the cycle.
(b) With the phase pulling of (3), the rate of approach to synchrony depends linearly on the strength of the coupling; with FTM, it is essentially a property of the oscillator alone, once the trajectories are close enough to be in case 1a (see Remark 2.2).

3 Rapid synchrony in one-dimensional arrays

3.1 Motivation for choice of simulation

We now consider one-dimensional arrays of oscillators to understand what features of the oscillators and/or their coupling are implicated in the ability to synchronize quickly. Specifically, we are interested in comparing the synchronization properties of large populations of oscillators whose coupling behavior is governed by fast threshold modulation with the synchronization properties of populations of oscillators whose behavior is governed by phase pulling. As we shall show in the simulations and explain heuristically, the FTM mechanism is expected to be significantly better at fast locking of long arrays.

We make this comparison by modifying the relative time scales of the internal variables of the oscillators in the array. We introduce two oscillator models, a single cell conductance-based model due to Morris and Lecar (1981) and a network-based oscillator model due to Ellias and Grossberg (1975).

The Morris–Lecar equations have the general form

$$\begin{aligned} dv/dt &= -g_{Ca} m_\infty(v)(v-1) - g_K w(v - v_k) \\ &\quad - g_L(v - v_L) + I_{ext} , \\ dw/dt &= \lambda[w_\infty(v) - w]/\tau_w(v) , \end{aligned} \quad (4)$$

where

$$\begin{aligned} m_\infty(v) &= 0.5[1 + \tanh\{(v - v_1)/v_2\}] , \\ w_\infty(v) &= 0.5[1 + \tanh\{(v - v_3)/v_4\}] , \\ \tau_w(v) &= 1/\cosh\{(v - v_3)/(2v_4)\} . \end{aligned}$$

We will analyze the simplest version of the Ellias–Grossberg equations, namely

$$\begin{aligned} dx/dt &= -Ax + (B - x)\{C[x - \Gamma]^+ + I_{ext}\} \\ &\quad - Dx[y - \Gamma]^+ , \\ dy/dt &= E(x - y) , \end{aligned} \tag{5}$$

where $[s]^+ \equiv \max(s, 0)$. The variable x represents the potential of an excitatory cell governed by a nonlinear shunting equation (Grossberg 1968, 1973; Sperling and Sondhi 1968); y represents the potential of an inhibitory cell governed by a linear equation. The parameters for (4) are: $v_1 = -0.01$, $v_2 = 0.15$, $v_3 = 0.1$, $v_4 = 0.145$, $g_{CA} = 1.0$, $g_L = 0.5$, $g_K = 2.0$, $v_L = -0.4$, $v_K = -0.7$. I_{ext} ranged from 0.05 to 0.15 in different trials. The parameters for (5) are $A = 1$, $B = 1$, $C = 20$, $D = 33.3$, $\Gamma = 0.4$. I_{ext} ranged from 1.0 to 2.0 in different trials.

For the Morris–Lecar (M–L) oscillator (4), the parameter λ (the relative rate at which conductance change occurs in the K^+ activation channel) provides control of the relative time scales. For instance, when λ is set to a small value, a single oscillator typically exhibits a plateau-like waveform (see Fig. 6a). Under these conditions we say that the oscillator is in its relaxation regime. However when λ is set to larger values (K^+ conductance changes more rapidly) the oscillator exhibits a more sinusoidal waveform (see Fig. 6b). Under excitatory chemical synaptic coupling, as in Sect. 2, the mechanism of fast threshold modulation governs the behavior in the relaxation regime. In the sinusoid regime, general invariant manifold theory suggests that phase-pulling mechanisms dominate the behavior (see Remark 3.1 below). Thus the oscillators we use can be modulated to exhibit FTM or phase-pulling behavior. Such a modulation may be achieved, for example, by changing the temperature of the neural preparation (Cole et al. 1970). Neuromodulators and pharmacological blockers are also known to be able to change the waveform of a neural oscillator (e.g., Harris-Warrick and Flamm 1987).

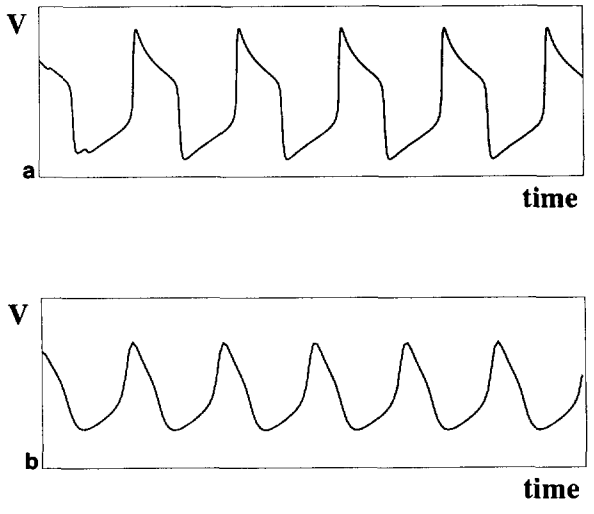

Fig. 6a, b. Morris–Lecar waveforms. **a** Relaxation waveform for M–L with $\lambda = 0.02$. **b** Sinusoid waveform for M–L with $\lambda = 0.33$

For the Ellias–Grossberg (E–G) oscillator, the parameter E in (5) governs the relative time scales of x and y and represents the relative rate at which the inhibitory interneuron tracks the firing rate of the excitatory cell. When E is small and thus (5) is in its relaxation regime, the excitatory cell exhibits a spike-like waveform and when E is near unity the excitatory cell exhibits sinusoid behavior.

Remark 3.1: For the sinusoidal regime, provided the coupling is not "too strong", invariant manifold theory can be used to reduce the full equations to ones dependent only on the phases of the oscillators (Ermentrout and Kopell 1990). Under further conditions, including weak coupling or other special considerations (Kopell and Ermentrout, 1991), the equations can be further simplified to ones depending only on phase *differences*. The function of the phase difference ϕ is not in general $\sin \phi$ as in (3). If the second simplification cannot be done, the behavior of an array of oscillators is not well understood, though some recent work has addressed this issue for globally coupled arrays (Golomb et al. 1992; Tsang et al. 1991). It also is known that one possible behavior is the cessation of all periodicity due to the interactions (Ermentrout and Kopell 1990). In giving our heuristic explanation, we are implicitly assuming that the equations we are simulating in the sinusoidal regime behave so that the averaging procedure used to produce equations depending only on phase differences yields equations whose behavior is that of the full system.

It was shown in (Kopell and Ermentrout 1986) that a chain of oscillators coupled via phase-differences does not generically approach synchrony. Rather, for long chains, the solutions approach travelling waves, with a boundary layer on one end. (The sinusoidal coupling of (3) is a special case for which synchrony does occur; a small perturbation, replacing $\sin \phi$ by $\sin \phi + A \cos \phi$, destroys the synchrony.) If the ends of the chain are coupled to form a circle, synchrony is robust for identical oscillators. (Travelling waves *can* form, however, for some initial conditions and we rejected those runs.) Since we are concerned here with the time scales of transients rather than the phase-lag pattern in the steady-state, we work with rings of oscillators and investigate approach to synchrony. (See Ermentrout, (1985) for more on rings of oscillators.)

This study of oscillator effects on synchronization is intended to complement the Grossberg and Somers (1991) study of network architecture effects on synchronization, and arose, in part, as a result of this prior study. Here we are interested in the rate at which synchrony can occur in a neural population which is sparsely connected. A limiting case of sparse connectivity is nearest neighbor coupling. This is the minimal network architecture that allows us to study the role of intrinsic oscillator properties on the speed of synchrony

in oscillator arrays. Nearest neighbor coupling is also interesting because recently it was argued mathematically that large, nearest neighbor chains of oscillators governed by some equations using phase difference coupling could not exhibit rapid synchronization (Kammen et al. 1989). These investigators concluded that nearest neighbor coupling was, *in general*, insufficient to generate rapid synchronization in a large population. Other researchers have concurred with this result using computer simulations of simplified oscillator models which explicitly implemented phase difference coupling (Baldi and Meir 1990; Niebur et al. 1991, Schuster and Wagner 1990). We show below in our computer simulations that nearest neighbor coupling is indeed capable of rapidly synchronizing large neural populations, when the coupling departs from phase-pulling behavior. Our result is consistent with recent reports that rapid synchronization can occur under local coupling alone (Grossberg and Somers 1991; König and Schillen 1991).

3.2 Computational methods

Computer simulations were run using 40 oscillators coupled in a nearest-neighbor ring geometry. Both the Morris–Lecar and the Ellias–Grossberg oscillators were simulated. The E–G simulations were based on those in Grossberg and Somers (1991). Earlier simulations of M–L were also done by Grossberg and Somers (unpublished results) in a different context. Numerical integration was performed with two fundamentally different algorithms, Runge–Kutta and Bulirsch–Stoer (Press et al. 1988), and thus it is unlikely that numerical error had a significant effect on our results.

For the M–L simulations, the ith oscillator was governed by (4), where v and w were replaced by v_i and w_i, respectively. Nearest neighbor coupling was implemented by adding the term

$$-\alpha[\tfrac{1}{2}g_{Ca}m_\infty(v_{i-1}) + \tfrac{1}{2}g_{Ca}m_\infty(v_{i+1})](v_i - 1)\,,$$

to the first equation in (4). For the E–G simulations, the ith oscillator was specified by (5) where x and y were replaced by x_i and y_i, respectively. Nearest neighbor coupling was implemented by adding the term

$$\alpha[B - x_i](\tfrac{1}{2}[x_{i-1} - \Gamma]^+ + \tfrac{1}{2}[x_{i+1} - \Gamma]^+)$$

to the first equation in (5).

For each simulation trial, the inputs and the coupling strength, α, were fixed, but were varied between trials. In order to compare the synchronization properties of sinusoid and relaxation arrays, the same initial phase conditions were set across the arrays in compared trials. To control for the effects of waveform differences (between the sinusoid and relaxation forms) on the coupling signal, α was scaled by a factor which normalized the total coupling input over a full cycle. In our simulations, this factor always enhanced the sinusoid coupling signal (α increased), and thus the results described below provide a more favorable case for the sinusoid array than if this factor had not been introduced.

Several hundred simulation trials were run, and in order to condense some of these results a statistical measure of phase coherence across the array was introduced. During a trial the times of the extreme peak and trough for each cycle of each oscillator were recorded. Phase coherence was computed on the basis of the standard deviation from mean of the times of the peaks and troughs, respectively, across the array for each cycle. The difference between each peak (or trough) time and the mean time was divided by the period so that a period-independent standard deviation was obtained. Phase coherence was defined such that 0 represents random phase incoherence and 1 represents synchrony: $\mathrm{PC} = 1 - (\mathrm{s.d.} \div \mathrm{s.d._{max}})$. A uniform distribution yields the maximal standard deviation:

$$\mathrm{s.d._{max}} = \left((2/(N-1))\sum_{i=1}^{N/2}(2i-1)^2/(2N)^2\right)^{1/2},$$

where N is the number of oscillators in the array. For $N = 40$, $\mathrm{s.d._{max}} \approx 0.2923$. Since phase coherence of the array was computed for both peaks and troughs of every cycle, two phase coherence measures per cycle were obtained. In order to control for dependence on initial conditions, the results of multiple trials were combined by computing the mean Phase Coherence across trials at each mean peak and trough. These results were used to form the plots of Fig. 8.

3.3 Simulation results

1. For a broad range of initial conditions and coupling strengths, one-dimensional arrays of relaxation oscillators synchronized more rapidly than did arrays of sinusoid oscillators under the same coupling and initial phase conditions. The absolute rates of synchronization, however, depend on the coupling strength. At a moderate coupling strength (e.g., $\alpha = 0.10$), the E–G and M–L relaxation, nearest neighbor networks almost always approached synchrony ($\mathrm{PC} > 0.8$) in four or fewer cycles, while it was uncommon for their sinusoid counterparts under the same conditions to approach this synchrony criterion in less than 30 cycles (see Fig. 7). Similar relative synchronization advantages were enjoyed under nearly every coupling strength tested.

For nearly all sets of initial phase conditions, the relaxation arrays exhibited rapid synchronization at some moderate coupling strength, while at moderate coupling strength the sinusoid arrays exhibited slow synchronization or no synchronization. The typical state for sinusoid networks after several cycles was reminiscent of shock waves across the array, with oppositely-directed travelling wave domains pieced together. Eventually (frequently after many, many cycles) this behavior would smooth out so that the phase difference between neighboring oscillators was approximately constant across the network, resulting in either synchrony or a uniform travelling wave. At low coupling strengths, the relaxation array sometimes rapidly formed into a uniformly spaced travelling wave or

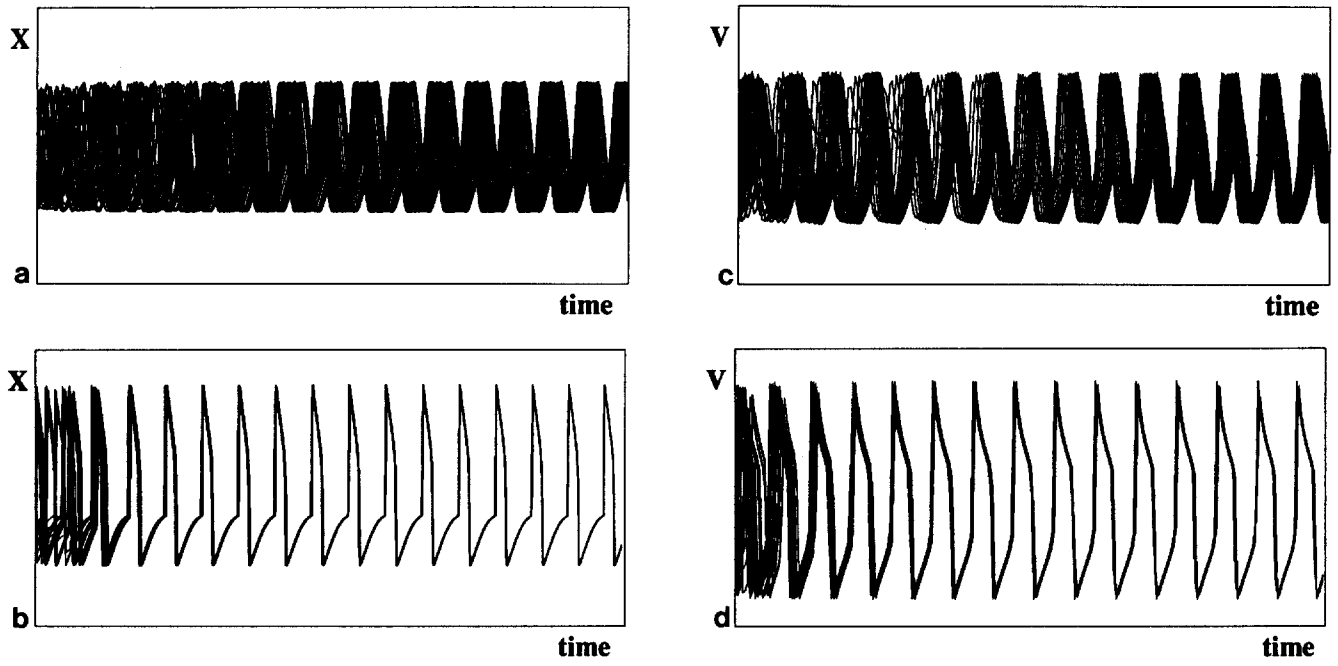

Fig. 7a–d. Relaxation arrays synchronize in many fewer cycles than do sinusoid arrays. The time courses of the 40 oscillators are overlaid in each graph. **a** and **b** compare typical synchronization behavior of the E–G oscillator in the sinusoid ($E = 1.0$) and relaxation ($E = 0.02$) regimes, respectively ($I_{Ext} = 1.0, \alpha = 0.1$). **c** and **d** compare typical synchronization behavior of the M–L oscillator in the sinusoid ($\lambda = 0.33$) and relaxation ($\lambda = 0.02$) regimes, respectively ($I_{Ext} = 0.1, \alpha = 0.1$). The random initial phase conditions were identical for the sinusoid and relaxation comparisons

formed into alternating regions of approximate synchrony and uniformly spaced travelling waves, and thus did not synchronize. In this latter case, behavior typically converged rather slowly to a uniformly spaced travelling wave. However, at moderate or higher coupling strengths, for nearly all conditions, this travelling wave behavior was replaced by rapid synchronization across the entire relaxation array. Figure 8 summarizes the sinusoid vs. relaxation results of the E–G and M–L oscillators for 25 sets of random phase initial conditions (ignoring initial conditions leading to travelling waves).

2. Rapid synchronization of the E–G oscillator array in the sinusoid regime was possible under very strong coupling (e.g., $\alpha \geqslant 1.0$). However, under these conditions the waveform closely resembled the relaxation waveform, which suggests that phase-pulling was no longer governing the behavior. This may be due, in part, to the explicit onset threshold, Γ, in the E–G equations.

3. Even under strong coupling, the M–L sinusoid array regularly failed to exhibit rapid synchronization. Instead, strong and often moderate coupling drove the sinusoid array into damped, rather than sustained oscillations, a phenomenon known as oscillator death (Ermentrout and Kopell 1990). Oscillator death was common to all of these oscillator forms, but this phenomenon always occurred at lower coupling strengths in the sinusoid than in the relaxation arrays. That is, arrays of relaxation oscillators have a greater ability to resist "oscillator death." For M–L, the relaxation array could typically withstand up to twice the coupling that the sinusoids could. This ability to sustain oscillations (i.e., resist oscillator death) under stronger coupling is additional synchronization advantage for relaxation arrays.

4. Nearest neighbor relaxation arrays consisting of oscillators with different natural frequencies could also be rapidly and tightly phaselocked to the same frequency with synchronized onsets and offsets even when the natural frequencies spanned an octave (factor of 2 range). Sinusoid arrays typically showed little phase-locking over the same frequency ranges. At higher coupling strengths the E–G sinusoid array could be nearly entrained, although phase relationships were not stable. Synchrony was not observed at coupling strengths for which the sinusoidal waveform was maintained.

5. In more fully connected architectures, relaxation arrays continued to enjoy a synchronization advantage. Although both sinusoid and relaxation arrays exhibited synchronization more rapidly as the number of connections was increased, the results suggested that the relative advantage of the relaxation oscillator arrays was comparable to that in the results presented above.

6. Under mild relaxation conditions (ϵ not near 0), the relaxation array would often rapidly achieve a state of near or "noisy" synchrony. The transition from random phase conditions to this noisy synchrony usually occurred in a small number of cycles; the transition from noisy synchrony to true synchrony was usually

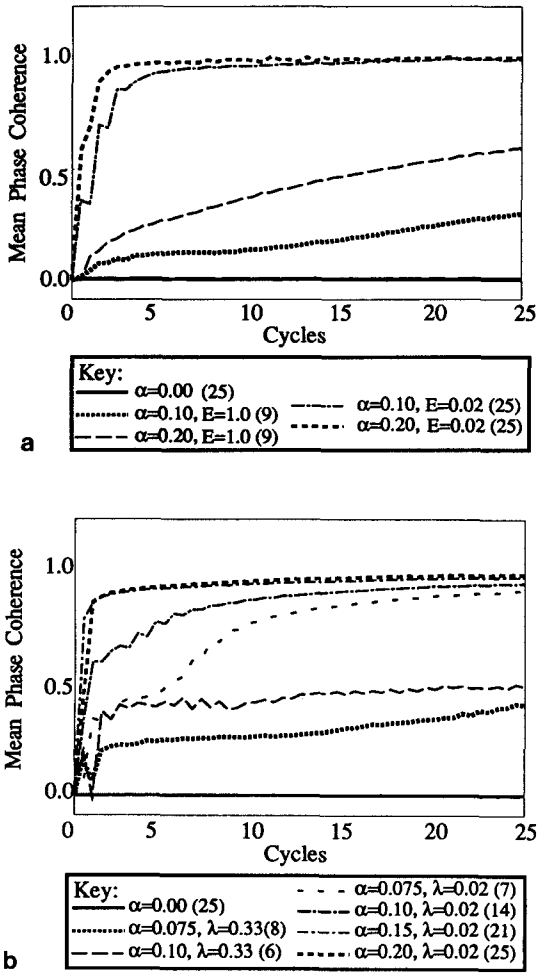

Fig. 8a, b. Relaxation array advantage in rapid synchronization occurs for a broad range of initial conditions and coupling strengths. The mean Phase Coherence (see Comp. Meth.) was computed for the sinusoid and relaxation forms of **a** E-G ($I_{Ext} = 1.0$) and **b** M-L ($I_{Ext} = 0.1$) for several different coupling strengths. The same 25 sets of initial phase conditions were tested for each group and the trials that eventually synchronized were used in the computation. The trial count is indicated in parentheses in the key. The M-L sinusoid arrays exhibited oscillator death for $\alpha = 0.15$, 0.20 and thus there is no data for them

rather slow (see Fig. 7d). This is consistent with the mechanisms described in Sect. 3, where it was shown that for points $O(\epsilon)$ away from synchrony a different rate of approach to synchrony was to be expected than for points $O(1)$ apart. As ϵ (λ in (4) or E in (5)) was increased and each oscillator was less strongly relaxation-like, the width of this noisy band increased, but the transition from noisy to true synchrony occurred at a more rapid rate.

3.4 Heuristic explanation

As seen from the above simulations, the oscillators in the relaxation regime synchronized dramatically faster. We now wish to suggest an explanation. In Sects. 2 and 3, we examined the features of oscillators that affect the ability of a *pair* of oscillators to synchronize. For a pair of oscillators, neither threshold modification nor phase-pulling is always superior; the outcome depends on coupling strength and/or properties of the oscillators. However, we suggest that for long arrays, the FTM mechanism is superior because of different *scaling properties* with respect to length of the array.

To support our conjecture, we first consider the FTM case, in the limit of instantaneous jumps. Suppose that some contiguous subset of a one-dimensional array has reached approximate synchrony, and an oscillator at one end of this subset receives a change of input due to a jump from a neighboring oscillator outside the subset. If the phase difference between the subset and the neighbor is not too large (i.e., falls into case 1a), the change in input causes the end oscillator of the subset to jump; if the coupling is uniform along the chain, this creates a change in input to the next, again causing an immediate jump. By this reasoning, the entire subset executes a jump simultaneously. Thus, the differential input to the end oscillator of the subset does not cause that oscillator to pull apart from the others in the subset: approximate synchrony is maintained, and even enhanced by the compression that occurs across the jump. For an array with initial conditions consisting of clumps of approximate synchrony with class 1a phase differences between clumps, this suggests that the rate of approach to synchrony should be bounded below independent of the size of the clumps and number of clumps. Thus a fast approach to synchrony is possible even for long arrays.

For more general initial conditions, the situation is more complex. For example, consider the case of two contiguous oscillators with the same phase having a in class 1b or 1c phase difference with a neighboring one. If the latter is ahead, its jump changes the input into one of the two initially synchronous oscillators, but does not immediately cause a jump of either. Instead, it causes the initially synchronous oscillators to travel along two different cubics. The successive jump of one of the two may then lead to the jump of the other, but because of the difference in speeds along the two cubics, the oscillators end up with different values of the slow variable, and hence different phases. That is, initially, synchronous oscillators can be pulled apart by some kinds of differential input. However, if the differences in velocity along the two cubics is not too great, and the compression is strong enough, these oscillators will be back to approximate synchrony after another jump, so they are not pulled apart for long. We conjecture that for a fixed coupling strength, there is a lower bound on the rate of approach to synchrony (for those trajectories that do approach synchrony, or at least some large subset of them) independent of the length of the array.

For $\epsilon \neq 0$, this conjecture cannot be true as stated since (e.g., with pure Heaviside coupling) a change of input at one end of an initially synchronous subset would take time at least $O(\epsilon)$ between each pair to propagate. We conjecture that the rate of approach is proportional to the number of oscillators, with a proportionality constant that tends to zero with ϵ.

We now contrast that behavior with the synchronization behavior in arrays of phase oscillators coupled through phase differences. We give evidence for a conjecture that the rate of approach to synchrony scales differently with the size of the array than oscillators coupled through FTM. We start with a generalization of equations of the form (3), extended to a one-dimensional array connected in a ring. Reduction procedures using averaging and invariant manifolds transform equations involving very general oscillators and coupling to ones coupled by some function of phase difference ϕ (Ermentrout and Kopell 1984; Kopell and Ermentrout 1991). This function is some 2π-periodic function $H(\phi)$, not in general $\sin\phi$. Stability of the synchronous solution requires that $H'(\phi) > 0$ for some interval of phase differences around $\phi = 0$. The equations for the phases $\{\theta_k\}$ are

$$\theta_k' = H(\theta_{k+1} - \theta_k) + H(\theta_{k-1} - \theta_k), \tag{6}$$

with θ_{N+1} identified with θ_1.

It is shown in (Kopell and Ermentrout 1986) that the equations for the phase differences $\phi_k \equiv \theta_{k+1} - \theta_k$ approach a continuum limit as $N \to \infty$. This continuum limit is

$$\phi_t = \frac{1}{N}\left\{[f(\phi)]_x + \frac{1}{N}[g(\phi)]_{xx}\right\}, \tag{7}$$

where $2f(\phi) \equiv H^+(\phi) + H^-(-\phi)$ and $2g(\phi) \equiv H^+(\phi) - H^-(-\phi)$, $0 \leqslant x \leqslant 1$ and $\phi(k/N) \approx \phi_k$. (The continuum limit was shown to be valid for time independent solutions.)

The right hand side of (7) has a convection-like term $[f(\phi)]_x$ and a diffusion-like term $[g(\varphi)]_{xx}$. Numerical simulations of (6) for a ring suggest that the trajectories first (on an $O(1)$ time scale) tend to form subdomains on each of which ϕ is approximately constant, with shock-like transitions between the subdomains. (Note that $\phi =$ constant is a solution to the "outer equation" $0 = [f(\phi)]_x$ of the time-independent version of (7).) This is subject to the ring constraint that $\sum \varphi_k$ be a multiple of 2π. In general, convection and diffusion terms operate differently on transition regions. The convection term, which has a time scale $0(N)$, tends to move the position of the transition layer; the diffusion term, which has the time scale $0(N^2)$, tends to reduce the differences between the constants at the edges of the subdomains. Thus, (7) suggests that the approach to synchrony occurs on the time-scale $0(N^2)$, which is much slower than the scale suggested above for the relaxation case.

We note that it may take considerable mathematical work to turn our heuristic explanations into a rigorous proof.

4 Discussion

4.1 Relation to pulse-coupled oscillators

We return to a system of two relaxation oscillators, coupled through FTM. As discussed above, the system is essentially uncoupled between jumps. Hence, the jumps could be regarded as pulses that change the position of the other oscillator. The situation, however, is considerably more complex than that of phase oscillators coupled through pulses (Mirollo and Strogatz 1990). One essential difference is that the jump of one oscillator changes the phase space of the other (i.e., the cubic along which it moves); until a particular periodic solution is specified using pieces of the available cubics (such as the trajectory of the synchronous solution), the notion of phase is not well-defined and it does not make sense to describe the effect in terms of a phase-response curve.

One periodic orbit of special interest is the synchronous trajectory. As seen above, for small differences in phase, the jump of one oscillator advances the other along this trajectory. For some larger initial phase differences, one cannot define the phase difference after the first oscillator has made its jump until the second one has also made its jump a finite time later. At that time, both oscillators have advanced in phase, though the phase difference between them may or may not have decreased. Thus, it is not natural to describe even this situation in terms of pulses from one oscillation that change the phase of the other.

The second periodic solution, with an unexpected mathematical mechanism, is the antiphase solution. This solution, which is discussed in detail in Kopell and Somers (1993), can occur stably if the time along the left branch of the upper cubic and the time along the right branch of the lower cubic are unequal. With non-equal branches, there are ranges of initial conditions (labeled in Sect. 2 as class 1d) in which one oscillator jumps onto and off of the shorter branch before the second has had a chance to jump at all. It is possible to derive a pulse response curve description of the dynamics in which one compares the position of oscillator 2 after the return of oscillator 1 (to the longer branch) to where oscillator 2 would have been without the excursion of oscillator 1. The difference is due to the fact that, while oscillator 1 is on its other branch, oscillator 2 moves along a shifted cubic, and hence moves at a different rate. For classes of neural oscillators like the ones we have been describing, with coupling mimicking excitatory chemical synapses, the effect of the excursion of oscillator 1 is to *delay* oscillator 2. As shown in Kopell and Somers (1993), under a convexity condition that holds for M–L and E–G, this leads to stable antiphase behavior, with a trajectory that is very different from the synchronous solutions. When the time spent along the right and left branches differs by a greater amount the domain of the antiphase solution is larger, although the rate of convergence may be decreased. The mathematical mechanism responsible for the antiphase solution (with purely excitatory coupling) is very different from that of Schöner and Kelso (1988) or Sherman and Rinzel (1992).

4.2 Oscillator properties can affect network behavior

Our simulation results for arrays of oscillators in Sect. 3 clearly suggest a caveat for the construction of net-

works of oscillators: the choice of the oscillators may significantly affect the phase locking properties of the network. In particular, conclusions (Kammen et al. 1989) drawn from some models using phase pulling about the network connectivity required for rapid synchronization do no generalize.

The simulations and arguments we have presented point to two types of distinctions that are relevant to network behavior. One is the distinction between phase models and relaxation oscillators coupled by fast modulation of the threshold. The second is a more subtle distinction among different kinds of relaxation oscillators. More specifically, we showed that (in the relaxation regime) oscillators with conductance-based features have properties that make them more efficient at synchronization than simple non-conductance based caricatures such as FitzHugh–Nagumo. The latter distinction is not expected to affect scaling properties.

The coupling we used was chosen to mimic excitatory chemical synaptic coupling with no significant delay. If the coupling has another form (e.g., electrical) or delays are significant, the conclusions of the analysis and the simulations may not hold. This reinforces our warning that models need to be carefully matched to the motivating context.

4.3 Transition between phase pulling and FTM

We argued in Sect. 3 that for different ranges of parameters the oscillators we use could be in a phase-pulling regime or an FTM coupling regime. The behavior for intermediate values of the parameter is much less understood and may turn out to be very model-dependent. As mentioned in Sect. 3, as ϵ increases, a larger band of phases is involved in "noisy synchrony", furthermore, the interactions during the jumps assume a successively larger role, leading eventually to phase pulling (in which there is a continuous interaction over the cycle).

4.4 Neuromodulation and the feature binding problem

In light of our findings, the fact that neurons can be modulated between sinusoid and plateau or spiking behavior suggests a potential role for neuromodulators in governing network synchronization. Application of a modulator to a cell population or subpopulation could facilitate rapid phase-locking behavior in that population. Since the timing of neural activity has been suggested to play an important role in functions such as development, rhythmic motor control, and the perceptual coding of visual (e.g., Eckhorn et al. 1988; Gray et al. 1989; Gray and Singer 1989), auditory (e.g., von der Malsburg and Schneider 1986), and olfactory (e.g., Freeman 1991) information, such a modulatory mechanism could have significant behavioral consequences.

The possible role of synchronized neural activity in coherent visual perception has attracted quite a bit of interest (e.g., Baldi and Meir 1990; Grossberg and Somers 1991; Kammen et al 1989; König and Schillen 1991; Niebur et al. 1991; Schuster and Wagner 1990; Sompolinsky et al. 1990) due to reports that visual cortical neurons exhibit oscillatory activity and that spatially distributed groups of these neurons display rapid synchronization in a stimulus-specific manner (Eckhorn et al. 1988; Gray et al. 1989; Gray and Singer 1989). In perception, sensory neurons can be viewed as localized feature detectors. This prevalent view leaves unsolved the problem of binding spatially distributed sensory features into globally coherent percepts. This problem is known as the "feature binding" problem. It has been suggested that feature binding may be performed by the stimulus-specific synchronization of visual cortical neurons. Moreover, it has been suggested that cortical information coding, in general, may be expressed by resonant standing waves in which cooperatively linked cells oscillate synchronously (Grossberg 1976, 1978, 1982). Attaining rapid synchronization is critical for this binding hypothesis, as perceptual coherence occurs on the order of hundreds of milliseconds. In a changing sensory environment, coherence must occur rapidly or it may not occur at all.

In the context of this synchronized binding hypothesis, our findings suggest a new, possible mechanism for "attentional searchlight" processing (e.g., Treisman 1982; Treisman and Gelade 1980) in coherent perception. If rapidly synchronized neural activity plays a critical role in coherent perception, then attention could modulate perception through the release of neuromodulators that change the intrinsic neural behavior at the locus of attention in ways that facilitate synchrony. Thus objects in regions outside the attentional focus may fail to achieve perceptual coherence in a dynamic and adapting sensory environment, while those objects attended to may be rapidly perceived as coherent. We wish to emphasize that ability to synchronize can be affected by changes in intrinsic properties of the oscillators or oscillating networks, in addition to changes of synaptic strength as used by Crick (1984) in his searchlight mechanism.

Acknowledgments. The first author wishes to thank S. Grossberg for his patient support. The work of the paper was inspired partially by conversations with L. Abbott.

References

Baldi P, Meir R (1990) Computing with arrays of coupled oscillators: An application to preattentive texture discrimination. Neural Comput 2:458–471

Cole KS, Guttman R, Bezanilla F (1970) Nerve excitation without threshold. Proc Natl Acad Sci (USA) 65:884–891

Crick F (1984) Function of the thalamic reticular complex: the searchlight hypothesis. Proc Natl Acad Sci (USA) 81:4586–4590

Eckhorn R, Bauer R, Jordan W, Brosch M, Kruse W, Munk M, Reitbock HJ (1988) Coherent oscillations: A mechanism of feature linking in the visual cortex? Biol Cybern 60:121–130

Ellias SA, Grossberg S (1975) Pattern formation, contrast control, and oscillations in the short-term memory of shunting on-center, off-surround networks. Biol Cybern 20:69–98

Ermentrout GB (1985) The behavior of rings of coupled oscillators. J Math Biol 23:55–74

Ermentrout GB, Kopell N (1984) Frequency plateaus in a chain of weakly coupled oscillators, I. SIAM J Math Anal 15:215–237

Ermentrout GB, Kopell N (1990) Oscillator death in systems of coupled neural oscillators. SIAM J Appl Math 50:125–146
FitzHugh R (1961) Impulses and physiological states in models of nerve membrane. Biophys J 1:445–466
Freeman WJ (1991). The physiology of perception. Sci Am 264 (2):78–85
Golomb D, Hansel D, Shraiman B, Sompolinsky H (1992) Clustering in globally coupled phase oscillators. Phys Rev A 45:3516–3530
Gray CM, König P, Engel A, Singer W (1989) Oscillatory responses in cat visual cortex exhibit intercolumnar synchronization which reflects global stimulus properties. Nature 338:334–337
Gray CM, Singer W (1989) Stimulus-specific neuronal oscillations in orientation columns of cat visual cortex. Proc Natl Acad Sci (USA) 86:1698–1702
Grossberg S (1968) Some physiological and biochemical consequences of psychological postulates. Proc Natl Acad Sci (USA) 60:758–765
Grossberg S (1973) Contour enhancement, short-term memory, and constancies in reverberating neural networks. SIAM 52:217–257
Grossberg S (1976) Adaptive pattern classification and universal recording, II: Feedback, expectation, olfaction, and illusions. Biol Cybern 23:187–202
Grossberg S (1978) A theory of visual coding, memory, and development. In: Leeuwenberg E, Buffart H (eds) Formal theories of visual perception. Wiley, New York
Grossberg S (1982) Studies of mind and brain: neural principles of learning, perception, development, cognition, and motor control. Reidel Press, Boston
Grossberg S, Somers D (1991) Synchronized oscillations during cooperative feature linking in a cortical model of visual perception. Neural Networks 4:453–466
Harris-Warrick R, Flamm R (1987) Multiple mechanisms of bursting in a conditioned bursting neuron. J Neurosci 7:2113–2128
Kammen DM, Holmes PJ, Koch C (1989) Cortical architecture and oscillations in neural networks: Feed-back versus local coupling. In: Cotterill RJM (ed) Models of brain function. Cambridge University Press, Cambridge, pp 273–284
König R, Schillen TB (1991) Stimulus-dependent assembly formation of oscillatory responses: I. Synchronization. Neural Comput 3:155–166
Kopell N, Ermentrout GB (1986) Symmetry and phaselocking in chains of weakly coupled oscillators. Comm Pure Appl Math 39:623–660
Kopell N, Ermentrout GB (1990) Phase transitions and other phenomena in chains of coupled oscillators. SIAM J Appl Math 50:1014–1052
Kopell N, Ermentrout GB (1991) Multiple pulse interactions and averaging in systems of coupled neural oscillators. J Math Biol 29:195–217
Kopell N, Somers D (1993) Pulse coupling, bistability, and fractured synchrony in arrays of relaxation oscillators (In preparation)
Malsburg C von der, Schneider W (1986) A neural cocktail-party processor. Biol Cybern 54:29–40
Mirollo RE, Strogatz SH (1990) Synchronization of pulse-coupled biological oscillators. SIAM J Appl Math 50:1645–1662
Mishchenko EF, Rozov N Kh (1980) Differential equations with small parameters and relaxation oscillations. Plenum Press, New York
Morris C, Lecar H (1981) Voltage oscillations in the barnacle giant muscle fiber. Biophys J 35:193–213
Nagumo J, Arimoto S, Yoshizawa S (1962) An active pulse transmission line simulating nerve axon. Proc IRE 50:2061–2070
Niebur E, Kammen DM, Koch C (1991) Phase-locking in 1-D and 2-D networks of oscillating neurons. In: Schuster HG (ed) Nonlinear dynamics and neuronal networks. VCH Weinheim, pp 173–203
Press WH, Flannery BP, Teukolsky SA, Vetterling WT (1988) Numerical recipes in C: the art of scientific computing. Cambridge University Press, Cambridge, pp 566–597
Schöner G, Kelso JAS (1988) A synergetic theory of environmentally specified and learned patterns of movement coordination, II. Biol Cybern 58:81–89
Schuster HG, Wagner P (1990) A model for neuronal oscillations in the visual cortex. 2. Phase description of the feature dependent synchronization. Biol Cybern 64:83–85
Sperling G, Sondhi MM (1968) Model for visual luminance discrimination and flicker detection. J Opt Soc Am 58:1133–1145
Sherman A, Rinzel J (1992) Rhythmogenic effects of weak electrotonic coupling in neuronal models. Proc Natl Acad Sci (USA) 89: 2471–2474
Sompolinsky H, Golomb D, Kleinfeld D (1990) Global processing of visual stimuli in a neural network of coupled oscillators. Proc Natl Acad Sci (USA) 87:7200–7204
Treisman A (1982) Perceptual grouping and attention in visual search for features and for objects. J Exp Psychol Hum Percept Perform 8:194–214
Treisman A, Gelade G (1980) A feature integration theory of attention. Cogn Psychol 12:97–136
Tsang KY, Mirollo RE, Strogatz SH, Wiesenfeld K (1991) Dynamics of a globally coupled oscillator array. Physica D 48:102–112